Proceedings of the International Conference on Oxide Materials for Electronic Engineering (OMEE 2021)

On Collective Interparticle Effects Underlying Unusual Coercive Behavior of Ensembles of Substituted Manganite Nanoparticles

A.I. Tovstolytkin[a,b,*], O.I. Nakonechna[a,b], I.V. Sharay[a], A.V. Bodnaruk[c], O.V. Bondar[c], V.M. Kalita[c,d], S.M. Ryabchenko[c], Y.Y. Shlapa[e], S.O. Solopan[e] and A.G. Belous[e]

[a] *Institute of Magnetism of the NAS of Ukraine and MES of Ukraine, 36-b Vernadsky Blvd., 03142 Kyiv, Ukraine*
[b] *Taras Shevchenko National University of Kyiv, 64/13 Volodymyrska str., 01601 Kyiv, Ukraine*
[c] *Institute of Physics of the NAS of Ukraine, 46 Nauky Ave., 03028 Kyiv, Ukraine*
[d] *National Technical University of Ukraine "Igor Sikorsky Kyiv Polytechnic Institute", 37 Peremohy Ave., 03056 Kyiv, Ukraine*
[e] *V.I. Vernadskii Institute of General and Inorganic Chemistry of the NAS of Ukraine, 32/34 Palladin Ave., 03142 Kyiv, Ukraine*

Doi: 10.12693/APhysPolA.141.351 *e-mail: atov@imag.kiev.ua

Temperature-dependent magnetic properties and spin echo decay behavior have been studied for an ensemble of $La_{1-x}Sr_xMnO_3$ ($x = 0.23$) nanoparticles (of 30 nm in diameter) synthesized by the sol–gel method. Characteristic magnetic parameters, such as blocking temperature and effective Curie temperature for the ensemble, are determined. Enhanced coercivity and its unusual temperature dependence compared to bulk counterparts are revealed, and possible reasons for this phenomenon are discussed. A conclusion about the non-negligible role of interparticle interactions in the enhancement of the coercivity in the ensembles of substituted manganites is made.

topics: magnetic hyperthermia, manganite nanoparticles, coercive force, spin echo decay

1. Introduction

Magnetic nanoparticles (MNPs) have now become necessary elements in the most important scientific fields like bioengineering, biomedicine, clinical therapy applications [1], bio-separation [2], magnetic resonance imaging (MRI), magnetically targeted drug delivery and magnetic hyperthermia (MHT) cancer therapy [3–5]. There is continuing interest in MHT as a complementary oncological treatment. In the medical field, cancer MHT refers to the use of magnetic-field-induced heat (typically 42–46°C) to slow down or stop tumor growth without affecting the normal tissues.

Recently, Sr-doped perovskite manganite (La,Sr)MnO_3 has been attracting interest for MHT applications due to relatively high heating efficiency and capacity for long-term maintenance of heating temperature at a preset level [6–12]. The Curie temperature of these compounds, which sets the upper limit of the AC-magnetic-field-induced heating temperature, can be easily tuned, and this makes substituted manganites promising for self-controlled MHT applications. The advantage of such applications consists in a strong reduction of the risk of overheating and damage to surrounding tissues [6, 13, 14].

Numerous experiments have shown that the properties of nanoscale manganites strongly differ from those of the bulk ones [15–17]. As a rule, microcrystalline and single crystalline samples display relatively weak coercivity, and there is no evidence of hysteretic behavior at room temperature. On the contrary, the manganite nanoparticle ensembles demonstrate enhanced coercivity, which persists up to the room and higher temperatures [17–19]. To date, however, little attention has been paid to the details of the coercivity behavior in the ensembles of substituted manganite nanoparticles and to the analysis of the processes contributing to the coercivity enhancement.

In this work, we analyze the results of magnetostatic and nuclear quadrupole/ nuclear magnetic resonance (NQR/NMR in internal hyperfine field of magnetically ordered crystal) measurements carried out on an ensemble of Sr-doped manganite MNPs, highlight unusual features of the coercivity behavior and show that interparticle interactions can contribute to the enhancement of coercivity in such kind of objects.

2. Materials and methods

Nanoparticles of lanthanum–strontium manganite $La_{1-x}Sr_xMnO_3$ with $x = 0.23$, denoted as LSMO in the rest of the text, were synthesized by the sol–gel method according to the route described in [20, 21]. At the final stage of the synthesis, the nanoparticles were heat treated at 800°C for 2 h.

The details of the MNP characterization were described in [22–24]. XRD data indicated that LSMO MNPs are characterized by a distorted perovskite structure with $R\bar{3}c$ space group and lattice parameters $a = 5.491(1)$ Å, $c = 13.363(2)$ Å, $V = 348.94$ Å^3 [14], where V is the volume of a lattice cell. Transmission electron microscopy data showed that the average MNP size is ~ 30 nm.

Magnetic measurements were performed using an LDJ-9500 vibrating sample magnetometer. NMR measurements were carried out in the internal field of nanopowders using the method of nuclear spin echo. An ISSh-2 NQR/NMR spin echo spectrometer was used in the two-pulse spin echo mode ($\pi/2$ and π) (the Khan method). Details of the magnetostatic and NQR/NMR measurements were described in our earlier papers [25, 26].

3. Results and discussion

Figure 1 shows field dependence of magnetization, $m(H)$, obtained at different temperatures for the LSMO nanopowder under investigation. It is seen that each $m(H)$ curve can be separated into two regions: within the first one ($H < 1.5$ kOe) magnetization is characterized by a high rate of growth, while within the second one ($H > 2$ kOe), it demonstrates a tendency to saturation. Analysis of the $m(H)$ curves makes it possible to determine characteristic magnetic parameters of the ensemble, such as effective Curie temperature T_C^{eff}, and coercive force H_c.

The approach to describe the behavior of MNP ensembles with relatively strong dispersion in magnetic parameters was developed in [25]. Theoretical background for the concept of using the effective Curie temperature for the ensemble of nanoparticles (T_C^{eff}) was substantiated. It was shown that at low temperatures, not far from T_C^{eff}, the saturation magnetization of the ensemble displays critical behavior and obeys scaling laws. At the same time, in close vicinity of T_C^{eff}, the magnetization vs temperature behavior deviates from the predicted one. The value of T_C^{eff} can be obtained by means of extrapolation of a low-temperature part of the $m(T)$ dependence to abscissa axis. The use of such procedure to the ensemble of LSMO nanoparticles studied in this work gives $T_C^{eff} \approx 335$ K.

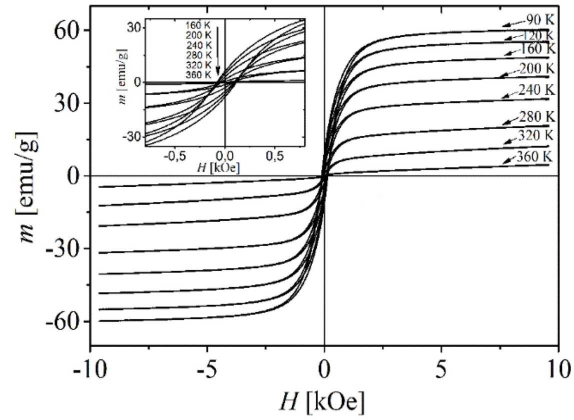

Fig. 1. Magnetization curves $m(H)$ in the range of magnetic fields of ± 10 kOe. The inset shows parts of the hysteresis loops in the range of ± 0.8 kOe fields.

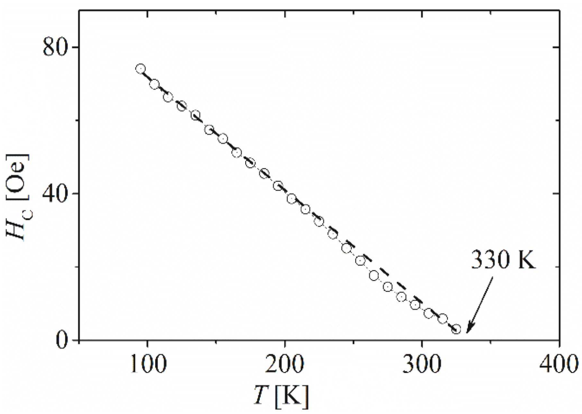

Fig. 2. Temperature dependence of the coercive force $H_c(T)$.

The analysis of the low-field parts of $m(H)$ dependence provides information about the behavior of coercive force for the ensemble of LSMO MNPs. One should note that for the case of ideal Stoner–Wohlfarth particles, the temperature dependence of coercive field obeys the law

$$H_c(T) = H_c(T = 0) \left(1 - \left(\frac{T}{T_b}\right)^{\delta}\right), \qquad (1)$$

where T_b is the blocking temperature and $\delta = 0.5$ [27]. As seen in Fig. 2, H_c for manganite MNPs obeys the same law with $T_b \approx 330$ K, but with $\delta = 1$. It is not surprising that $\delta \neq 0.5$ for manganite nanoparticles, because the magnetization of nanoparticles exhibits quite strong changes with temperature (see Fig. 1) and does not remain constant, as assumed in the Stoner–Wohlfarth model.

The behavior of $m_{FC}(T)$ and $m_{ZFC}(T)$ is in compliance with that of $H_c(T)$, i.e., with an increase in temperature, the curves start to coincide at around 330 K (Fig. 3). This serves as additional confirmation that blocking temperature $T_b \approx 330$ K.

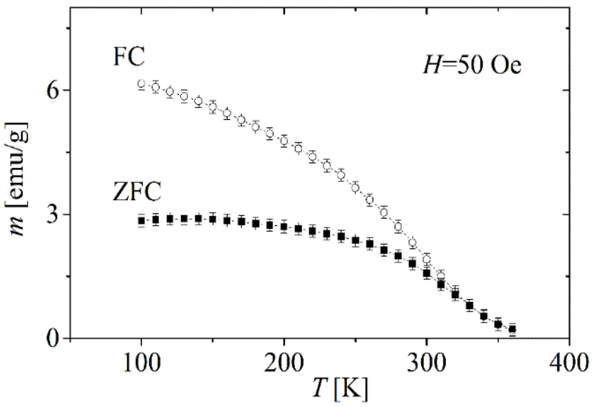

Fig. 3. Measurement data according to FC and ZFC protocols. Temperature dependence for magnetizations $m_{\mathrm{FC}}(T)$ and $m_{\mathrm{ZFC}}(T)$ measured in a field $H = 50$ Oe.

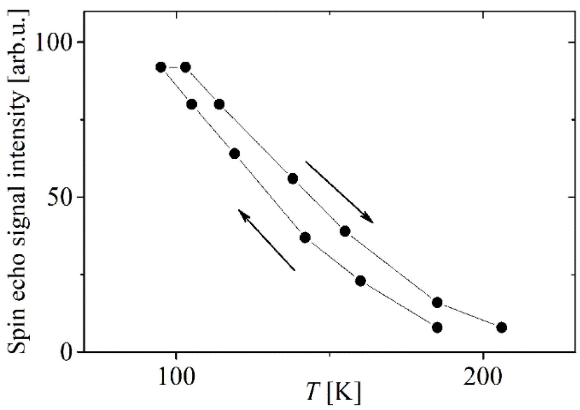

Fig. 4. Temperature dependence of the intensity of the ^{139}La spin echo signal from the demagnetized LSMO nanopowder (measurements started from a high temperature).

As was noted in the Introduction, bulk perovskite manganites have relatively weak anisotropy and display low coercive behavior. At the same time, the ensembles of *nanoscale* manganites show highly coercive behavior up to sufficiently high temperatures (often up to the effective Curie temperature), as demonstrated in this and other works [17–19, 28]. Although some ideas about the origin of this phenomenon have been suggested [29–31], one point, namely the contribution of interparticle interactions, has not been properly analyzed yet.

An important question requiring the explanation is: can we expect that the effect of interparticle interactions can exert a non-negligible influence on the magnetic parameters of the ensemble of particles if the particles are located close to one another? One way to answer this question is to measure the temperature dependence of the transverse relaxation time T_2 of nuclear magnetic resonance in the internal field of the magnetically ordered state of particles.

For substituted manganites, such resonance can be observed for ^{55}Mn and/or ^{139}La nuclei, whose spins are nonzero and are affected by the spins of the electron shell of Mn ions by a hyperfine interaction. One of the characteristics of NQR, NMR, and/or NMR in the internal hyperfine field of magnetically ordered crystal is the transverse relaxation time T_2, which can be measured using the spin echo method [26]. It should be noted that T_2 is the time of preservation of the coherence of the precessing nuclear spins in the mentioned hyperfine field after the system gets excited with a short radio pulse having a resonance frequency. Naturally, the fluctuations in the magnitude of the hyperfine field associated with thermally activated fluctuations in the directions of the magnetic moment of particles at temperatures above T_{b} will lead to a sharp reduction in T_2. And for very short T_2 values, the spin echo signal becomes difficult to observe, even with the smallest admissible time delays between excited and reading pulses.

NQR/NMR measurements of the spin echo of ^{139}La nuclei were carried out on the powders studied in this work. The spectral dependence of the amplitude of spin echo signal on ^{139}La has one very wide line that continuously overlaps the frequency range of 5–25 MHz. Upon the cooling of the powder, the signal becomes observable below 200 K. A quite unexpectable feature is that the temperature dependence of the signal amplitude displays a noticeable hysteresis with a 10–15 K width, i.e., the signal amplitude turns out substantially lower in the mode of cooling the sample down to a rather low temperature (~ 100 K) than that obtained while heating it from this minimal temperature (Fig. 4).

The following explanation of the observed phenomenon is possible. At temperatures above T_{b}, the hyperfine field of the Mn electron shells fluctuates rapidly due to thermally activated changes in the directions of the magnetic moments of the particles. Therefore, the signals of the spin echo on ^{139}La are not observed — the time T_2 for them is extremely short. The cooling of the sample to the temperatures below blocking temperature results in the fixation of the magnetization direction of every particle into a definite direction. On the one hand, this results in a sharp increase in T_2, which makes the spin echo signal detectable. On the other hand, the magnetized single domain particles interact through their dipole fields and, being free for mechanical displacements, are expected to form larger conglomerates. The particles are actually no longer independent, single domain ones, and upon the heating, they exhibit spin echo signal amplitude, which is different from that observed upon the cooling. In order to unblock the collective configuration of the directions of the magnetic moments of neighboring particles, it is necessary to increase the temperature above the initial T_{b} of individual particles. It will break the magnetic bond of the particles and make the particles behave independently.

It follows from the above experiments that the cooling of the ensemble of LSMO MNPs leads to the enhancement of interparticle interactions and may eventually result in the formation of the collective configurations of the directions of the magnetic moments of neighboring particles. These processes will not affect such parameters as saturation magnetization and effective Curie temperature, but it is expected that they will make a non-negligible contribution to the coercivity of the ensemble.

4. Conclusions

Magnetostatic and NQR/NMR measurements on the ensemble of $La_{1-x}Sr_xMnO_3$ ($x = 0.23$) nanoparticles synthesized by the sol–gel method (average particle size is near 30 nm) have been performed. It is found that the effective Curie temperature for the ensemble is approximately equal to 335 K, and the blocking temperature is around 330 K.

Temperature dependence of coercive force was analyzed. It has been shown that the coercive force falls almost linearly with temperature and drops to zero near the blocking temperature. It is stressed that the values of H_c exceed those reported for bulk $La_{1-x}Sr_xMnO_3$ samples.

It is found that the temperature dependence of the spin echo signal amplitude displays a noticeable hysteresis with a 10–15 K width, i.e., the signal amplitude turns out substantially lower in the mode of cooling the sample down to a rather low temperature than that obtained in the mode of heating it from this minimal temperature. It is concluded that this effect originates from the formation of collective configurations of the directions of magnetic moments of neighboring particles at low temperatures caused by enhanced interparticle interactions. This effect will not influence such parameters as saturation magnetization and effective Curie temperature but is expected to make a non-negligible effect on the transformation of the coercivity behavior of the ensemble.

Acknowledgments

The work is partially supported by the Ministry of Education and Science of Ukraine (Project No. 0121U110014) and the National Academy of Sciences of Ukraine (Projects 0117U001915 and 0122U002260).

References

[1] E. Pollert, K. Zaveta, in: *Magnetic Nanoparticles from Fabrication to Clinical Applications*, Ed. Nguyen T.K. Thanh, CRC Press, Boca Raton 2012, p. 449.

[2] P.A. Liberti, C.G. Rao, L.W.M.M. Terstappen, *J. Magn. Magn. Mater.* **33**, 301 (2001).

[3] N.D. Thorat, R. Bohara, in: *Nanoarchitectonics for Smart Delivery and Drug Targeting*, Eds. A.M. Holban, A. Grumezescu, William Andrew, App. Sci. Publishers 2016, p. 589.

[4] K. El-Boubbou, *Nanomedicine* **13**, 953 (2018).

[5] I.M. Obaidat, B. Issa, Y. Haik, *Nanomaterials* **5**, 63 (2015).

[6] A.K. Pradhan, R. Bah, R.B. Konda, R. Mundle, H. Mustafa, O. Bamiduro, R.R. Rakhimov, *J. Appl. Phys.* **103**, 07F704 (2008).

[7] S. Vasseur, E. Duguet, J. Portier et al., *J. Magn. Magn. Mater.* **302**, 312 (2006).

[8] K. Zhang, T. Holloway, J. Pradhan, M. Bahoura, R. Bah, R.R. Rakhimov, A.K. Pradhan, R. Prabakaran, G.T. Ramesh, *J. Nanosci. Nanotechnol.* **10**, 5520 (2010).

[9] K.R. Bhayani, S. Arora, R. Rajagopal et al., *Nanotechnology* **18**, 345101 (2007).

[10] N.D. Thorat, V.M. Khot, A.B. Salunkhe, R.S. Ningthoujam, S.H. Pawar, *Colloids Surf. B* **104**, 40 (2013).

[11] N.D. Thorat, S.V. Otari, R.M. Patil, R.A. Bohara, H.M. Yadav, V.B. Koli, A.K. Chaurasia, R.S. Ningthoujam, *Dalton Trans.* **43**, 17343 (2014).

[12] N.D. Thorat, V.M. Khot, A.B. Salunkhe, A.I. Prasad, R.S. Ningthoujam, S.H. Pawar, *J. Phys. D Appl. Phys.* **46**, 105003 (2013).

[13] E. Pollert, K. Knížek, M. Maryško, P. Kašpar, S. Vasseur, E. Duguet, *J. Magn. Magn. Mater.* **316**, 122 (2007).

[14] N.K. Prasad, K. Rathinasamy, D. Panda, D. Bahadur, *J. Biomed. Mater. Res. B Appl. Biomater.* **85**, 409 (2008).

[15] V.M. Kalita, A.F. Lozenko, S.M. Ryabchenko, P.O. Trotsenko, A.I. Tovstolytkin, A.M. Pogorily, *Ukr. J. Phys.* **54**, 157 (2009).

[16] Y. Suzuki, H.Y. Hwang, S-W. Cheong, T. Siegrist, R.B. van Dover, A. Asamitsu, Y. Tokura, *J. Appl. Phys.* **83**, 7064 (1998).

[17] P. Dey, T.K. Nath, *Appl. Phys. Lett.* **89**, 163102 (2006).

[18] S. Daengsakul, C. Thomas, C. Mongkolkachit, S. Maensiri, *Solid State Sci.* **14**, 1306 (2012).

[19] V.M. Kalita, A.F. Lozenko, S.M. Ryabchenko, A.A. Timopheeev, R.A. Trotsenko, I.A. Danilenko, T.E. Konstantinova, *Low Temp. Phys.* **34**, 436 (2008).

[20] S.O. Solopan, O.I. V'yunov, A.G. Belous, T.I. Polek, A.I. Tovstolytkin, *Solid State Sci.* **14**, 501 (2012).

[21] Y. Shlapa, S. Solopan, A. Belous, A. Tovstolytkin, *Nanoscale Res. Lett.* **13**, (2018).

[22] V.M. Kalita, D.M. Polishchuk, D.G. Kovalchuk, A.V. Bodnaruk, S.O. Solopan, A.I. Tovstolytkin, S.M. Ryabchenko, A.G. Belous, *Phys. Chem. Chem. Phys.* **19**, 27015 (2017).

[23] Y. Shlapa, M. Kulyk, V. Kalita, T. Polek, A. Tovstolytkin, J.-M. Greneche, S. Solopan, A. Belous, *Nanoscale Res. Lett.* **11**, 24 (2016).

[24] A.I. Tovstolytkin, A.M. Pogorily, D.I. Podyalovskii et al., *J. Appl. Phys.* **102**, 063902 (2007).

[25] A.V. Bodnaruk, V.M. Kalita, M.M Kulyk, S.M Ryabchenko, A.I Tovstolytkin, *J. Phys. Condens. Matter.* **31**, 375801 (2019).

[26] O.V. Bondar, V.M. Kalita, A.F. Lozenko, D.L. Lyfar, S.M. Ruabchenko, P.O. Trotsenko, I.A. Danilenko, *Ukr. J. Phys.* **50**, 823 (2005).

[27] J.M.D. Coey, *Magnetism and Magnetic Materials*, Cambridge University Press 2010.

[28] A. ur Rashid, S. Manzoor, *J. Magn. Magn. Mater* **420**, 232 (2016).

[29] P. Žvátora, M. Veverka, P. Veverka et al., *J. Solid State Chem.* **204**, 373 (2013).

[30] C. Aruta, G. Ghiringhelli, V. Bisogni, L. Braicovich, N.B. Brookes, A. Tebano, G. Balestrino, *Phys. Rev. B* **80**, 014431 (2009).

[31] S. Valencia, L. Peña, Z. Konstantinovic, Ll. Balcells, R. Galceran, D. Schmitz, F. Sandiumenge, M. Casanove, B. Martínez, *J. Phys. Condens. Matter* **26**, 166001 (2014).